Hard X-ray measurement during the current startup phase in QUEST

Saya TASHIMA[1], Hideki ZUSHI[2], Mitsutaka ISOBE[3], Shoichi OKAMURA[3], Hiroshi IDEI[2], Kazuaki HANADA[2], Sanjeev K. SHARMA[1], Tomofumi RYOUKAI[1], Masaki ISHIGURO[1], Haiqing LIU[1] and the QUEST group

[1] *IGSES, Kyushu University, Kasuga, Fukuoka, 816-8580, Japan*
[2] *RIAM, Kyushu University, Kasuga, Fukuoka, 816-8580, Japan*
[3] *National Institute for Fusion Science, 509-5292,Toki, Japan*

(Received: 30 October 2009 / Accepted: 31 March 2010)

ABSTRACT

Hard X-ray measurement (5 keV to 60 keV) has been performed in the current ramp-up phase of an electron cyclotron heated plasma in the spherical tokamak QUEST. The pulse height analysis of the hard X-ray is carried out with a fast time resolution of 1 ms, and the build-up of the spectrum and the evolution of the photon flux are studied under the various operation conditions (initial gas pressure, P_{gas}, RF power, P_{RF}, and vertical magnetic field, B_z). The parameter dependence of the X-ray is compared with that of the driven plasma current, I_p. The fast time responses of the X-ray and I_p in P_{gas} and P_{RF} scans are coincident with each other at the breakdown, and time averaged values during the discharge show a similar dependence on P_{gas} and P_{RF}. In the B_z scan I_p shows a peak at the optimal B_z, however, both the temperature and flux of the hard X-ray (Γ_{HX}) spectrum show minima near the same B_z. The B_z dependence of I_p is discussed.

Keywords; Hard X-ray, Electron cyclotron resonance heating, Current start-up, Electron Bernstein wave, Mode conversion, Spherical tokamak, Relativistic effects

1. Introduction

In a spherical tokamak one of the most urgent issues for steady state operation is the establishment of non-inductive current start up and sustainment methods. Pressure-driven current (bootstrap current) and electron Bernstein current drive EBCD are promising candidates and a number of non-inductive current drive experiments have been carried out in CDX-U[1], DIII-D[2], LATE[3] and MAST[4]. Although the current start-up must be performed in an open magnetic field configuration combined with the toroidal, B_t, and vertical, B_z, fields, the initial condition of the poloidal fields must provide a modicum of confinement. In references a weak mirror field configuration has been chosen to confine on initial slab plasma produced by ECW. Although the existence of energetic electrons has been confirmed after the closed flux surfaces have been formed in LATE[5] and CPD[6], it is not clear whether energetic electrons can contribute to the initial toroidal current in the open field or not. In the present paper the hard X-ray (HXR) measurement was used to compare with the time evolution and the following parameter dependences of the initial I_p. Special emphasis was placed on the contribution of energetic electrons to net toroidal current before the closed magnetic surfaces have been formed.

Four mechanisms are considered for a net toroidal current in the open fields, i.e., 1) a toroidal return current (Pfirsh-Schlüter current) compensating the charge separation caused by the ∇B and curvature drifts v_d, 2) a toroidal precession current caused by the banana orbits of the trapped electrons, 3) a toroidal circulating current carried by so-called stagnated very high energy electrons whose vertical component of the parallel velocity $v_{\|z}$ is balanced by v_d [7], and 4) a parallel diamagnetic current, so-called bootstrap current in the open field. Since these currents (1, 2, 4) have similar dependences on the electron pressure (pressure gradient), and vertical (poloidal) field, the validation of mechanisms must be carefully done. The observed dependence of the sign (positive) of B_z on the toroidal direction (negative) of I_p satisfies the same requirement for all mechanisms. In this paper, the details of the B_z dependence of I_p were studied from the view point of quasi poloidal equilibrium balancing the $E \times B$ outward loss and the parallel loss along the field lines to the wall [8,9]. The anisotropic electron distribution effect ($v_{\|} << v_{\perp}$) on the B_z dependence was also analyzed. The dependence of the collision frequency on I_p was also investigated from the view point of the collisionless nature of energetic electrons whose collisionality is required to be in the banana regime. This paper is organized as follows. Section 2 describes the spherical tokamak QUEST device[10], heating and current drive system, HXR diagnostics and experimental conditions. The results of the parametric study will be presented in Section 3. The role of energetic electrons on

author's e-mail: tashima@triam.kyushu-u.ac.jp

the initial I_p is discussed and a summary is given in Section 4.

2 EXPERIMENTAL SETUP

2-1 QUEST device

QUEST is a medium sized spherical tokamak device. The device parameters of the QUEST chamber without a toroidal cut are as follows. The outer and inner diameters of the chamber are 0.2 m and 1.4 m, respectively, and the height is about 2.8 m. Two flat divertor plates are set at ± 1 m from the mid-plane. The major (R_0) and minor (<a>) radii of the plasma are 0.68 m and 0.4 m, respectively. Eight toroidal magnetic field coils (TF coil) can produce 0.29 T at R=0.5 m in steady state. The poloidal magnetic field is generated by five sets of mirror coils (PF coils). Two RF waves at f_{RF} = 2.45 GHz (<50 kW, continuous operation) and f_{RF} = 8.2 GHz (<200 kW, continuous operation) are used for these experiments. For 2.45 GHz, waves are launched from the low field side in the O-mode, and for 8.2 GHz both O- and X-modes can be injected. They are injected on the mid-plane.

2-2 HXR diagnostics

Two semiconductor detectors (CdZnTe and CdTe) with 3×3×2 and 3×3×1 mm^3 are used to measure HXR in the energy range up to 1 MeV. The detection efficiency (> 0.3) of the detectors covers the range of 3 - 200 keV. The energy calibration was performed using three radioactive gamma-ray sources (I^{129}, Cs^{137}, Co^{60}). Pulse height analysis (PHA) is used to obtain the energy spectra integrated along the tangential chords on the mid plane, as shown in Fig.1. Tangency radii, R_{tan}, are 0.372 m (CdZnTe) and 0.5 m (CdTe), respectively. The diameter of the viewing area is ~ 0.3 m at the plasma center, which is decided by an aperture with the diameter of 5 mm in front of the detectors. The collimator made of tungsten is used. Two kinds of PH analyzer with dwell times from 1 to 100 ms are used to measure the time evolution of spectra during the discharge up to 1.1 s.

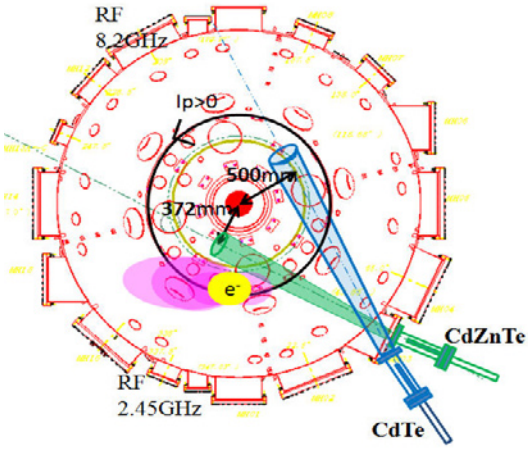

Fig.1 Top view of QUEST with HX diagnostics. 8.2 and 2.45 GHz ports are also shown.

The shaping time of the pulses is 1-3 μs for the PHA. Raw signals of pulses are also recorded every 0.2 μs to study the fast response of HXR just after the RF waves are injected. Fast electrons collide with ions and bulk electrons and radiate in the HXR range of the spectrum. When the electron energy is high, the radiation lobes of bremsstrahlung emission strongly shift forward along the electron drift direction by the relativistic effect. Forward (backward) emission is detected by CdTe (CdZnTe) when I_p (>0) is driven in the CCW direction or the current carrying electrons flow in the CW direction.
The positive sign is defined in the positive ϕ direction in a cylindrical coordinate system (R, ϕ, Z), where R is the major radius of the torus.

2-3 Experimental conditions

In these experiments, the toroidal field is generated in the pulsed mode for ~ 1 s (8.25 GHz) or ~ 1.5 s (2.45GHz). B_z is applied at a certain value prior to the RF pulse and kept constant during the discharge. No loop voltage is induced at the beginning and during the discharge. The ratio of B_z/B_t is $<\pm 40\times10^{-3}$ at R = R_{res} for both 2.45 GHz and 8.2 GHz, and typical R_{res} values are 0.37 m (2.45 GHz) and 0.33 m (8.2 GHz), respectively. Fast camera imaging of the plasma shows that the boundary of the plasma is formed between R_{res} and $2R_{res}$ and an annular slab plasma is extended to the upper and lower divertors. The chamber temperature is kept at 40 - 70 °C and the base pressure is 9×10^{-5} Pa. Gas is fueled by a piezo valve at 100 - 200 ms prior to the RF pulse and the initial P_{gas} is controlled < 1×10^{-3} Pa by the width of the gas puffing τ_{Gas}. Then the RF waves are switched on to initiate plasma. For 8.2 GHz a low level power of 1 kW is applied prior to the main pulse, but no pre-ionization power is injected for 2.45 GHz.

3 EXPERIMENTAL RESULTS

3-1 HXR in a typical ECR discharge

Figure2 shows a typical discharge by 8.2 GHz, in which I_p is below a certain value of I_p^{jump}, which is an indication of the formation of the closed flux surfaces [3,7]. A rectangular waveform of H_α was observed, though external gas was not fueled during the pulse. This may be due to enhanced recycling from a less conditioned wall. Hence I_p was not increased during the pulse, and it was considered that a current jump did not occur under this wall condition. Constant I_p (~ - 0.8 kA) was driven in the CW direction. Since the measured HXR energy was lower than 12 keV, isotropic emission from electrons was detected by CdTe. A steady state of the energetic electrons was established during the whole discharge.

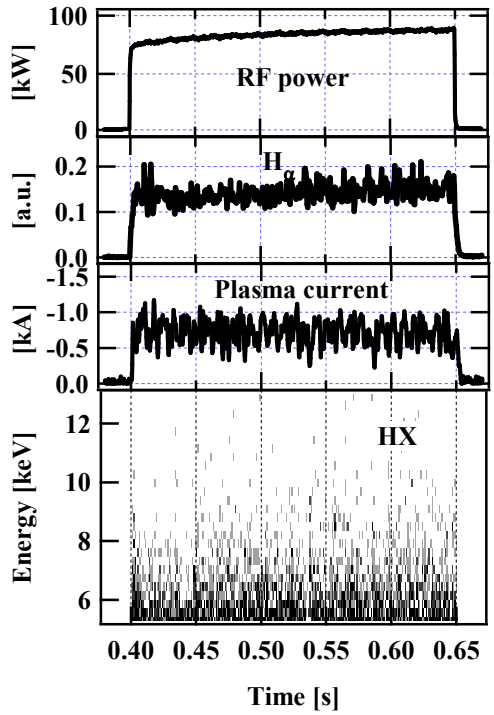

Fig.2 Typical discharge by ECRH(8.2 GHz). Waveforms of P_{RF}, I_p, H_α and HXR spectrum are shown.

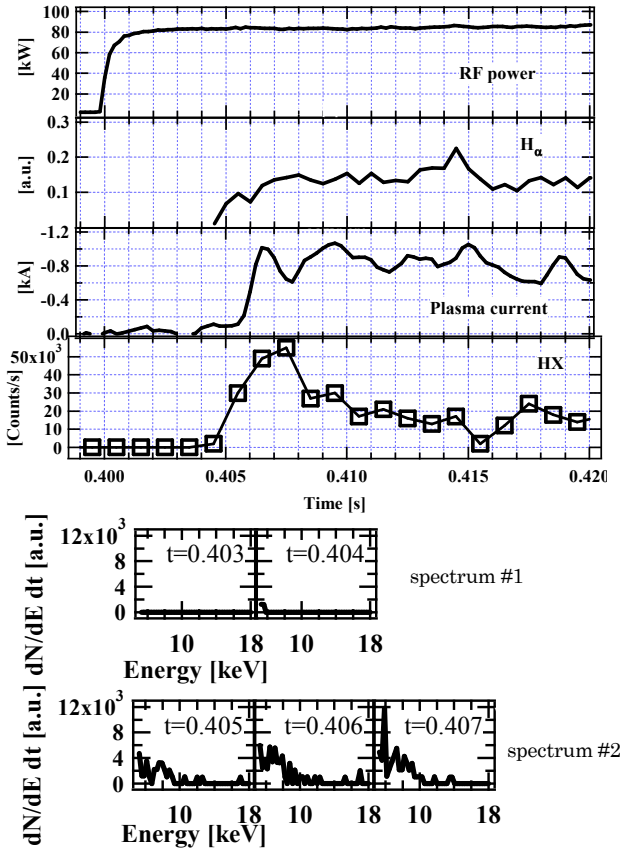

Fig.3 The evolution of P_{RF}, I_p, H_α and HXR spectrum for a time interval of 20ms.

3-2 The evolution of HXR in an expanded time scale

Since the wall condition in the present experiment is the "wall fueling" condition as indicated by H_α in Fig.2, the very fast phase of the plasma current generation is focused on. Abrupt rises in I_p and HXR spectrum were observed when plasma breakdown occurred. Figure 3 shows the evolution of P_{RF},H_α, I_p, and counts > 6keVfor 1 ms in the expanded time scale. The spectra for every 1 ms are also shown. Breakdown is delayed by ~ 4.5 ms at the source rate of ~ 5.4×10^{17} H_2/s. The spectra #1 (t = 0.403 to 0.404 s) shows no HXR (> 6 keV) before breakdown. On the other hand, spectra #2 (t = 0.405 to 0.407 s) show that generation of energetic electrons at the energy of > 6 keV is coincident with the breakdown. The maximum energy of 18 keV was observed. A positive correlation between the abrupt rises in I_p and HXR suggests that energetic electrons contribute to the formation of the plasma current because of their collisionless nature.

3-3 Initial gas pressure dependence

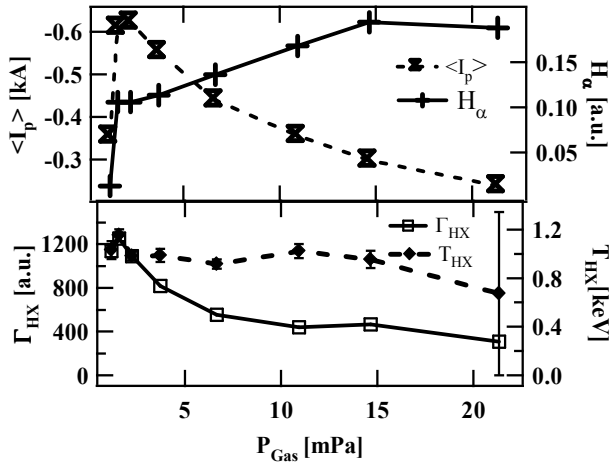

Fig.4 The P_{Gas} dependence of I_p, H_α the flux of HXR and the temperature of HXR.

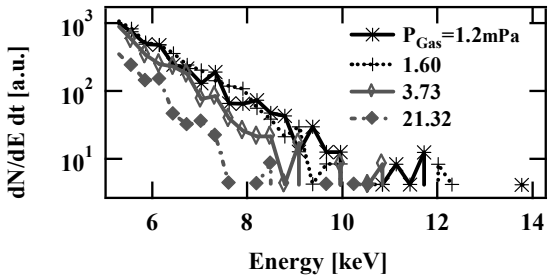

Fig.5 The HXR spectra as a function of P_{Gas}.

It has been reported in [1, 2, 11] that particle recycling strongly affects the performance of RF current drive. Here the collision effects on energetic electrons were investigated by a comparison between I_p and HXR. A gas pressure scan experiment is performed using 8.2 GHz waves at P_{RF} ~ 70 kW. P_{gas} in the chamber is changed from 1.2×10^{-3} to 2.1×10^{-2} Pa by varying the initial gas puff width(τ_{Gas}) from 15 ms to 0.3 s before discharge. The external pumping was stopped by closing valves just before each discharge. Other experimental conditions are fixed. At low P_{gas} the breakdown is delayed at fixed P_{RF} and magnetic configuration. By introducing the delay-times

(τ_{Ip}, τ_{HXR}) for I_p and HXR to start to rise with respect to the RF injection time the coincidence between τ_{Ip} and τ_{HXR} is observed as a function of P_{gas}. The result shows that τ_{Ip}, τ_{HXR} and $\tau_{H\alpha}$ are ~ 10ms at 1.2 mPa and become less than 2.3 ms above it. Figure 4 shows the P_{gas} dependence of I_p, Γ_{HX}, integrated in the energy range, and the slope ($\propto -1/T_{HXR}$) of the spectrum. These quantities are averaged during the discharge. Γ_{HX} is reduced with increasing P_{gas}, and I_p shows a similar tendency except at the lowest P_{gas}. Quantitative reduction factors for both I_p and Γ_{HX} as P_{gas} increases are similar, and the time response of both quantities is consistent with each other within 2 ms. Figure 5 shows the HXR spectra as a function of P_{gas}. Although T_{HXR} is almost constant except at the maximum P_{gas}, Γ_{HX} is reduced to 1/3. Although the observable maximum energy is down to ~ 8 keV, it is evidence that RF waves can still accelerate electrons at least up to ~ 8 keV at the maximum P_{gas} of 1.2×10^{-3} Pa. These relatively collision-less electrons, compared to the thermal electrons having less than a few tens of eV, can survive for a longer collision time, which may drive the current. Since both pressure dependences of Γ_{HX} and I_p are similar, these observations suggest that initial energetic electrons created by RF waves contribute to I_p, but collisional processes via neutrals including ions reduces I_p at this power level when P_{gas} is increased. The enhanced H_α during the discharge, indicating the pressure rise, also affects the I_p rise.

3-4 Power dependence

P_{RF} scan experiments have been carried out using 8.2 GHz waves from 20 to 90 kW at τ_{gas} of 50 ms. Other operational parameters are fixed. Waves are injected in mixed (both O and X-modes) modes and only the total power is varied. Figure 6 shows the P_{RF} dependence of $\tau_{H\alpha}$, τ_{Ip}, τ_{HXR} and the initial I_p. Here the initial I_p is defined as a current peak value at the breakdown phase. To avoid the enhanced recycling effects I_p at the beginning phase is used. At the lowest power of 20 kW τ_{Ip} is ~ 30 ms but I_p shows a sharp rise up to ~ 0.6 kA at the breakdown. No HXR > 5 keV is observed, though the lower energy component may be expected. HXR becomes observable when the P_{RF} exceeds 30 kW. τ_{HXR} is 90 ms ~ at 30 kW to less than 10 ms above 50 kW.

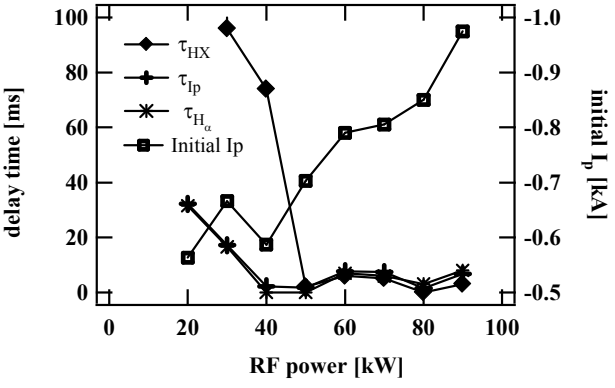

Fig.6 The features of breakdown by varying P_{RF}.

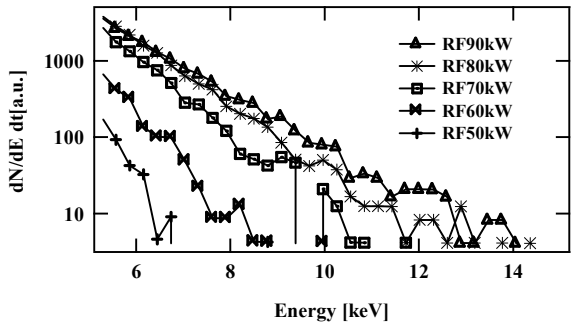

Fig.7 The HXR spectra as a function of P_{RF}.

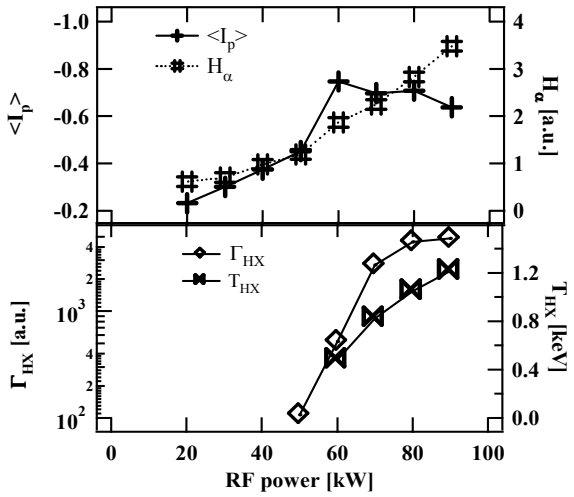

Fig.8 The P_{RF} dependence of I_p, H_α the flux of HXR and the temperature of HXR.

A similar tendency between them also supports the idea that energetic electrons contribute somewhat to I_p. The initial peak of I_p at the breakdown slightly varies from 0.6 to 1 kA. The time averaged spectra for 0.25 s are shown for various P_{RF} in Fig. 7. Below 50 kW, a spectrum with enough statistical accuracy was not achieved, but above it the P_{RF} dependence of the HXR spectrum is measured. For 50 – 70 kW the spectra increase in the whole energy range, however, above 80 kW, the increment in the higher energy range becomes significant. Figure 8 shows the P_{RF} dependence of I_p, H_α Γ_{HX} and T_{HXR}. T_{HXR} increases from 0.48 keV at a P_{RF} of 60 kW to 1.22 keV at 90 kW. However, Γ_{HX} increases by three orders of magnitude. The time averaged plasma current $<I_p>$ during the discharge is found to increase linearly with increasing P_{RF} for 20 kW < P_{RF} < 50 kW, and then it jumps at P_{RF} of 60 kW. A further rise in I_p is not obtained. Since enhancement in H_α with increasing P_{RF} is found, it is considered that the apparent saturation of Γ_{HX} at a P_{RF} of 70 kW is partially ascribed to the enhanced collision with neutrals.

3-5 B_z dependence

The effects of B_z on HXR are studied in two kinds of RF discharges at 2.45GHz and 8.2 GHz at the different B_t keeping the ratio B_z/B_t almost constant. For 2.45 GHz experiment P_{RF} is 4 kW and the steady plasma duration lasts for 1.1 s. R_{res} is fixed at 0.37 m and B_z is scanned from –3 mT to +3 mT. Since the annular slab plasma is

unstable and blob ejection at a typical frequency of ~ 1 kHz may affect I_p, the time averaged quantities (I_p and H_α) over the whole discharge duration are studied. In Fig. 9 (a) $<I_p>$ shows a semi-symmetric B_z dependence, whose peaks exist at $B_z/B_t = 0$ and $B_z/B_t \sim 1.2\times10^{-2}$. This small apparent positive shift of B_z/B_t is caused by mutual coupling of the used RF coils and unused closed ones. Actually $B_z/B_t=0.6\times10^{-2}$ seems to correspond to $B_z = 0$. H_α is also consistent with the optimal B_z, at which H_α reaches the maximum. The energy spectrum of HXR is taken every 0.1 s and it extends to ~ 65 keV. Since the energy spectrum is steady during the discharge, the time averaged one is analyzed. The T_{HXR} and Γ_{HX} show two minima corresponding to the maxima of $<I_p>$ as is shown in Fig. 9 (b,c).

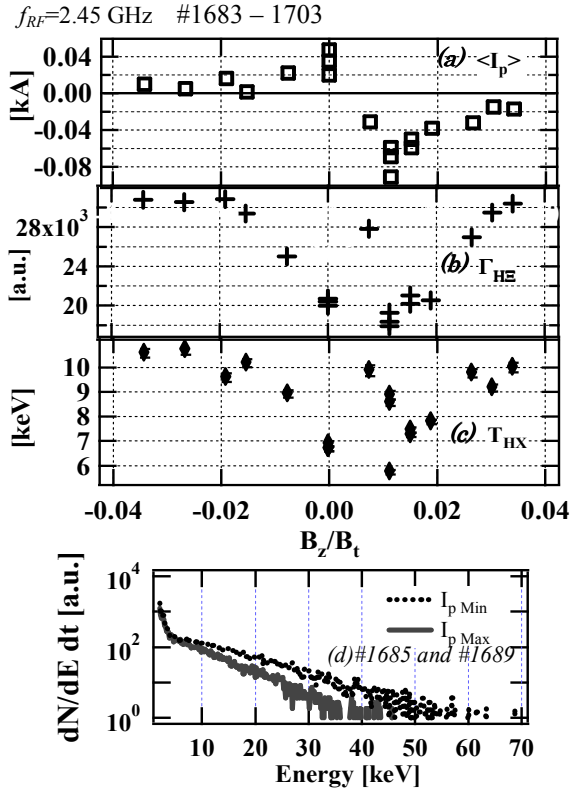

Fig. 9 (a)I_p , (b)Γ_{HX} and (c)T_{HX} vs. B_z/B and (d), the energy spectra at the minimum and maximum of I_p for f_{RF}=2.45GHz.

The similar B_z dependence is also investigated at 8.2 GHz at higher B_t of 0.293 T at R_{res} = 0.327 m, as show in Fig. 10 (a). Without mutual coupling problems the B_z scan could be carried out. The plasma duration is 0.13 s. P_{RF} is 60 kW. The $<I_p>$ absolute value is much larger than that of the 2.45 GHz data and a symmetric dependence is found. Although B_t is higher, the optimal B_z/B_t is in the same range. The energy range of the spectrum is reduced to ~ 15 keV, which is thought to be caused by the increased plasma cutoff density of 7.6×10^{17} m^{-3}. The minima of Γ_{HX} and T_{HXR} also agree with the maxima of $<I_p>$, as is shown in Fig. 10 (b,c). These B_z scan experiments suggest that there are two unresolved problems. One is the minima-maxima relation with respect to $<I_p>$. The energy spectra for 2.45 GHz and 8.2 GHz cases are compared at both I_p minimum and maximum, as is shown in Fig. 9 (d) and Fig. 10 (d), respectively. The other is the existence of HXR at $B_z = 0$. In this configuration no equilibrium exists and only very unstable plasma can be created. These points will be discussed later.

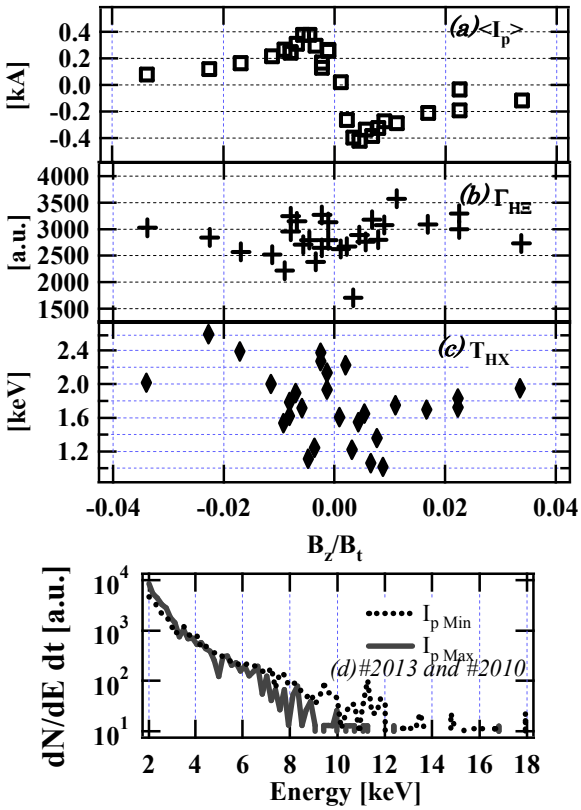

Fig. 10 (a)I_p , (b)Γ_{HX} and (c)T_{HX} vs. B_z/B. (d) The energy spectra at the minimum and maximum of I_p for f_{RF}=8.2GHz.

4. Discussion and summary

In order to study the contribution of the energetic electrons on initial current formation, parameter (P_{gas}, P_{RF}, and B_z) scan experiments of I_p and HXR are carried out.

Two P_{RF} and P_{gas} scan experiments are discussed by following simple momentum balance in which the source rate from RF waves is dissipated through collisions with both ions and neutrals.

$$\frac{dj}{dt} = \frac{e}{m}\frac{P_{RF}}{(\omega/k_\parallel)} - \nu_{ei+en} j \qquad (1)$$

,where $j = -enu_\parallel$ is the driven current density, ν_{ei+en} is the collision frequency of electrons with ions and neutrals, $\omega/k_\parallel$ the phase velocity of the injected waves, and e and m are the elementary charge and electron rest mass, respectively. When P_{gas} is increased from 3.7 to 14.7 mPa, Γ_{HX} is reduced to ~ 30 % and $<I_p>$ is also reduced by ~ 50 %. Since the neutral density, n_0, in the bulk plasma is not measured, n_0 is assumed to be increased by a factor of two, which is deduced from the variation in H_α. Since this enhancement in n_0 dominates the collisional dissipation, the driven current at the stationary state is expected to be reduced by a factor of two at constant P_{RF} if the resonance condition is not changed. By using data of T_e and n_e of 8 to

3 eV and 3 $\times 10^{17}$ to 0.5×10^{17}m^{-3}, which are measured near the wall, the thermal plasma contribution to $j \propto n_e\sqrt{T_e}$ is reduced to 10 %. Since T_{HX} is little changed within a few %, the energetic contribution on $j \propto n_{e-HX}\sqrt{T_{HX}}$ is ~ 50 % if n_{e-HX} is reduced by the same order. Here $n_{e\text{-}HX}$ is the density of energetic electrons. From the change in Γ_{HX}, which is proportional to the product of n_e and $n_{e\text{-}HX}$, a 50 % reduction in $n_{e\text{-}HX}$ is possible if n_e in bulk is reduced to ~ 60 %. Thus the energetic contribution is more plausible from the P_{gas} dependence of I_p. At constant P_{gas}, P_{RF} is varied from 50 kW to 90 kW. This causes both increments in I_p by 175 % and T_{HX} by ~ 400 %, respectively. It is observed that n_e and T_e near the wall increased from 0.2 to 1.7 $\times 10^{17}$m^{-3} and 1.5 to 5 eV, respectively. With an assumption of the same variation in bulk n_e and T_e as n_e and T_e near the wall, the thermal contribution to P_{RF}/ν_{ei} is evaluated ~125 %, on the other hand the high energy contribution is ~170 %. Thus, two scan data suggest that the contribution of energetic electrons to the plasma current is plausible. The detailed measurement of the bulk parameters is left to the future.

The confinement of current carrying particles (j/τ) is also considered in the right hand side of Equation 1 and the B_z dependence of I_p is analyzed along this line. According to a model of quasi poloidal equilibrium [8, 9], the following optimum B_z at which τ is maximized can be derived for a slab plasma whose width and height are Δ and h, respectively.

$$|B_{z,opt}| = \sqrt[3]{\frac{2\nu_{\parallel}B_t m_e\sqrt{MT_{\parallel}}}{Re^2}\frac{H}{\Delta}\left(1+\frac{T_{\perp}}{T_{\parallel}}\right)}, \qquad (2)$$

where $\nu_{\parallel}$, m_e, M, $T_{\parallel}$ and $T_{\perp}$ are parallel Coulomb collision frequency, electron and ion masses, parallel and perpendicular temperatures, respectively. Using $T_{\parallel} = T_{\perp}$ =10 eV, the cutoff density of 8×10^{17} m^{-3}, and H/Δ~ 10, the B_z dependence of τ_p is compared with data for 8.2 GHz. Agreement is quite good, as shown in Figure 11. The fast rise with increasing B_z is due to the rapid reduction in E×B outward loss by line tying effects and the slow decay above $B_{z,opt}$ is ascribed to the enhanced parallel wall loss. For 2.45 GHz the cutoff density of 7.4×10^{16} and B_t=0.0875 T give a similar value of $B_{z,opt}/B_t$ ~ 0.8 % , which is also consistent with that in Fig. 9. When we take into account the anisotropic temperature $T_{\perp}/T_{\parallel}$ of 10^3, the deviation from the dotted curve in Fig. 11 is within experimental variation, because $\nu_{\parallel}$ varies inversely with $T_{\perp}/T_{\parallel}$ [9]. Thus, one can expect that this quasi equilibrium is possible for energetic electrons with $T_{\perp} >> T_{\parallel}$ and their contribution to the initial current is larger than that of cold ones.

Based on a single particle drift picture in open fields, a profile of the toroidal precession current is arc-shaped, but that of stagnated current is circular. Since a slab plasma is formed, the bootstrap current is bipolar. The magnetic analysis using flux loops suggests that the current profile outside the last closed flux surfaces, especially on the outboard side of the torus, must be taken into account for reconstruction [6,12] even after the closed flux surfaces have been formed. If this is the case in the open fields, precise magnetic measurement will verify the contribution of stagnated circular passing electrons. This is left for the future.

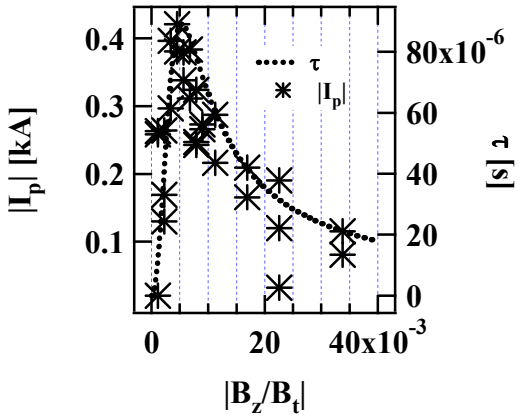

Fig.11 τ and $|I_p|$ dependence of $|B_z/B_t|$ for f_{RF} = 8.2 GHz.

In summary, we have examined the mechanisms during the current ramp-up phase of RF plasma in the open fields. HXR measurements suggest that energetic electrons play an essential role in carrying the current in this phase. The stagnated circulating electrons are one of the candidates to drive the current.

Acknowledgements

This work is supported by a Grant-in-Aid for Scientific Research (21246139). It is also partially performed with the support and under the auspices of the NIFS Collaboration Research Program (NIFS09KUTR041). S.T. would like to acknowledge Dr Y. Watanabe of Kyushu University for his kind help in the calibration of the detectors.

References

[1] C.B. Forest, et al., Phy. Rev. Lett. **68** (1992) 3559
[2] C.B. Forest, et al., Phys. Plasmas **1** (1994) 1568
[3] T. Maekawa. et al Nucl. Fusion **45** (2005) 1439
[4] V. Shevchenko, et al., Nucl. Fusion **50** (2010) 022004
[5] S.K. Sharma, et al., Nucl. Fusion **50** (2010) 025717
[6] H. Tanaka, et al., 22nd IAEA FEC, EX/P6-8 2008
[7]T. Yoshinaga, et al., Plasma and Fusion Res. series **8** (2009) 0100
[8] S. Nakao et al., Phys. Lett. **96**A (1983) 405
[9] S.H.Muller, et al., Phy. Rev. Lett. **93** (2004) 165003
[10] K. Hanada et al., 22nd IAEA FEC FT/P3-25,2008
[11] H. Zushi, et al., Nucl. Fusion **49** (2009) 055020
[12] M. Ishiguro et al., this conference